

RAS 8322

DOCKETED
USNRC

RESULTS OF THE FR2 IN-PILE TESTS ON LWR FUEL ROD BEHAVIOR

August 9, 2004 (11:45AM)

OFFICE OF SECRETARY
RULEMAKINGS AND
ADJUDICATIONS STAFFE.H. Karb¹⁾, L. Sepold¹⁾
P. Hofmann²⁾, C. Petersen²⁾, G. Schanz²⁾, H. Zimmermann²⁾Kernforschungszentrum Karlsruhe,
Hauptabteilung Ingenieurtechnik¹⁾
Institut für Material- und Festkörperforschung²⁾
Postfach 3640
D-7500 KarlsruheNOTICE: This material may be protected under the
Federal Republic of Germany
by copyright law (Title 17, U.S. Code)

ABSTRACT

Presented are the results of the FR2 In-Pile Tests on fuel rod behavior under LOCA conditions performed with PWR-type unirradiated and irradiated (2500 to 35000 MWd/t) fuel rods. The burst data do not indicate major differences from out-of-pile results. No influence of burnup on the burst data was observed. In the regions with major clad deformations of the pre-irradiated rods the fragmented fuel pellets were found crumbled within the fuel rod. The posttest examinations indicate clad mechanical behavior and oxidation to be comparable to out-of-pile results and a relatively small fission gas release during the transient.

OBJECTIVES, TEST PROGRAM

The in-pile experiments simulating the second heatup phase of a loss-of-coolant accident (LOCA) in a pressurized water reactor (PWR) were performed in the FR2 reactor at the Kernforschungszentrum Karlsruhe (KfK). The research is part of the Nuclear Safety Project's fuel behavior program. The main objective of the FR2 In-Pile Tests was to provide information about the effects of a nuclear environment on the mechanisms of fuel rod failure under LOCA conditions. The nuclear environment is characterized mainly by the genuine nuclear heat generation in UO₂ fuel.

The tests were conducted with unirradiated as well as with previously irradiated short-length single rods. The objectives of the program require a comparison with non-nuclear tests. Therefore, reference tests with electrically heated rod simulators were conducted in the in-pile loop under conditions identical to those of the nuclear tests. The entire test program is given in Table 1. The main parameter of the test program was the degree of burnup, ranging from 2,500 to a maximum of 35,000 MWd/t_U. As a second parameter the rod internal pressure was varied between 25 bars and 125 bars at steady state temperature. The pressure range used was larger than it is to be expected during the lifetimes of PWR rods. The desired pressure was adjusted during the preparations for the transient test by adding helium

NUCLEAR REGULATORY COMMISSION

Docket No. 50-413/414-01A Official Exh. No. 5 SH
In the matter of DUKE CATAWBA
Staff _____ IDENTIFIED 7/15/04 as E.C.D
Applicant ✓ RECEIVED _____
Intervenor _____ REJECTED _____
Cont'g Off'r _____ WITHDRAWN 7/15/04
Contractor _____ DATE _____
Other _____ Witness _____
Reporter Ruben Smith

TABLE 1: FR2 IN-PILE TESTS ON FUEL BEHAVIOR. TEST MATRIX

Type of Test	Test Series	Number of Rods Irradiated	Number of Tests	Target Burnup MWD/tt	Range of Internal Pressure at Steady State Temperature bar
Calibration, Scoping	A	-	5	-	25 - 100
Unirradiated Rods Main Parameters: Internal Pressure	B 1	-	7	0	55 - 90
	B 3	-	2	0	
Irradiated Rods Main Parameters: Burnup	C	6	5	2500	25 - 110
	E	6	5	8000	25 - 120
	F	6	5	20000	45 - 85
	G 1	6	5	35000	50 - 90
	G 2	2	2	35000	60 - 125
G 3	4	3	35000		
Electrically Heated Fuel Rod Simulators Main Parameters: Internal Pressure	BSS	-	8	-	20 - 110

to the fission gas generated during the previous irradiations. Heatup rates varied between 6 and 20 K/s.

EXPERIMENTAL CONDUCT

In each test the test rod is exposed to a standard temperature history derived from calculations for a PWR fuel rod under the conditions of the second heatup phase during a cold-leg break LOCA. The transient is initiated by interruption of the loop coolant flow and depressurization of the coolant. During the subsequent heatup phase the test rod power is kept constant until the target cladding temperature of approx. 1200 K is reached. At that temperature the rod power is rapidly reduced by reactor scram. The test procedure is given in Fig. 1.

The test rod internal pressure is adjusted prior to the transient. During the transient the gas is confined in the rod such that the internal pressure is measured but not controlled. The deformation and the burst of the rod cladding are monitored by means of the cladding temperature and rod internal pressure traces.

Cladding temperature was measured by six thermocouples resistance spot-welded to the rod surface at six different axial and azimuthal locations. Two different attachment versions (A and B) were used.

TEST RESULTS AND RESULTS OF NON-DESTRUCTIVE PTE **)

Burst Data

The burst temperatures are plotted versus burst pressures in Fig. 2. The data obtained from unirradiated and irradiated rods are indicated by different symbols. For comparison two dashed curves approximating the out-of-pile ORNL *) Multirod Burst Test single-rod results are included. There was no difference found between the burst data from unirradiated rods and those irradiated to the different burnups. Furthermore, burst pressures and burst temperatures measured during the in-pile tests lie within the data band obtained from out-of-pile experiments with electrically heated fuel rod simulators. This was confirmed by the results from the own simulator (BSS) tests being performed under identical conditions in the in-pile test loop. The BSS data are included in Fig. 2.

The definitions of burst temperature and burst pressure used in the evaluation of the FR2 In-Pile Tests are as follows: The burst temperature is defined as the temperature of the cladding at the burst location at burst time. It was determined by extrapolation from the thermocouple closest to the burst location. In order to compensate for the deviations of the surface-welded thermocouples a correction value was added. In this method azimuthal temperature variations cannot be taken into account.

The burst pressure is defined as the rod internal pressure measured at the beginning of the fast pressure drop, i.e., when the pressure gradient $\Delta p/\Delta t$ exceeds the value of minus 10 bars/s. The pertinent time after initiation of the transient is called burst time.

In Fig. 3 the measured maximum circumferential strains $\Delta U/U_0$ (burst strains) are plotted versus burst temperatures.

Here again the results from unirradiated and irradiated rods are indicated by different symbols. The three data points from the simulator (BSS) tests available to date are included in this diagram. The results from the FR2 In-Pile Tests lie in the range between 25 and 67 % circumferential strain. (The 67 % limit is reached when the deforming rod touches the shroud.) The results do not show an influence of irradiation on the burst strain and do basically correspond with the maximum deformations found in out-of-pile tests using an indirect heating of the cladding⁴, including tests performed with spent reactor fuel cladding.

A correction factor mentioned above was applied to the burst temperatures in Fig. 3. According to microstructural investigations of the cladding material (section 4.2) this factor could have been overpredicted for test rods using the thermocouple version A. In this case, some of the data points have to be shifted to somewhat lower temperatures in the diagram.

*) Oak Ridge National Laboratory, Oak Ridge, Tennessee (U.S.A.)

**) Post-Test Examination

Cladding Deformation Profiles

The axial strain profiles obtained with test series F (20,000 MWD/t burnup) are given in Fig. 4. The claddings exhibit deformation on the entire length (500 mm). The ballooned parts of the rods are located between 200 and 400 mm above the bottom of fuel stack, i.e. within the instrumented section of the rod. Fig. 4 shows also the normalized axial power profiles for each of the F-Tests. The position of maximum strain is usually at or close to the position of maximum rod power. However, the relatively flat power profile may have allowed other parameters, e.g. wall thickness, fuel eccentricity, increase of cladding mass and heat transfer surface by TC leads, to have influenced the position of maximum strain. Fig. 5 underlines this statement in demonstrating the random distribution of the position of maximum strain under conditions of extremely flat rod power profiles.

A cladding deformation extending to the 67 % limit at a length of about 10 cm was obtained with Test Rod E5. The strain profile and the post-test neutron radiograph of this rod are given in Fig. 6. An extension of the ballooning above 67 % was prevented by the shroud surrounding the test rod such that the cladding had to continue its ballooning into the axial direction. The deformation behavior of this test may be explained by the atypical test conduct (reactor scram at the onset of ballooning in contrast to the other tests) resulting in a cladding temperature decrease during the main part of the deformation and a delayed pressure release through a pin-hole opening in the cladding.

Fuel Condition

All tests with previously irradiated rods exhibited a fuel condition different from the experiments with unirradiated rods. As in commercial fuel rods the pellets in the test rods were cracked during operation at power and the fragments were held in place by the cladding. When, during the transient test, the cladding moved away from the fuel due to radial deformation, the pellet fragments filled the thus generated additional space. This led to a complete loss of pellet shape in the ballooned section and, for rods with larger deformation, to a significant reduction of the pellet stack height.

There was essentially no additional cracking of the fuel during the transient tests. This fact was clearly demonstrated by particle size analyses which resulted in similar size distributions for rods exposed to a transient and rods not exposed to such conditions after irradiation. Fig. 7 presents the results from the sieve analyses of the G1 fuel samples (burnup 35,000 MWD/t_F). The data of the reference rods not being exposed to a transient lie in the band of all other samples. The mean fragment size was measured to be about 0.3 cm.

From two tests (E3 and E4) it was learned that the fuel movement (pellet fragmentation) in the rod occurs in the moment of large deformation and burst of the cladding. Fig. 8 presents the cladding temperature and internal pressure histories during Test E4 and the special thermocouple instrumentation. Three thermocouples (T 137 through T 139) in these two tests were mounted at the upper end of the fuel stack in order to monitor the collapse of the pellet column. At the time of burst the three lower

thermocouples T 131 through T 133 behave as usual: A moderate temperature reduction indicates the increase of gap width and a flow of relatively cold plenum gas past the TC locations.

The severe temperature drops of the TCs T 137 through T 139, however, are a clear indication for the fuel movement leading to a reduction of the fuel stack of about 50 mm as could be evaluated from the posttest neutron radiographs.

RESULTS OF DESTRUCTIVE PTE

Analysis of Deformation of Zircaloy-4 Cladding

To describe quantitatively the complex nature of Zircaloy-4 deformation the method of the localization parameter W is used, where $0 \leq W \leq 1$. Small values indicate uniform and high values localized deformation.

The radial-strain localization parameter W_{θ} introduced by H.M. Chung and T.F. Kassner⁵ as calculated for series A, B, and F shows the same $W_{\theta}/\epsilon_{\max}$ correlation (Fig. 9) as the pertinent ANL data⁵ for directly heated cladding tubes. However, the W_{θ} values of the in-pile tests are 5 to 15 % higher than the ANL data.

A comparison of the axial-strain localization parameter W_z between the in-pile tests of series A, B, and F and out-of-pile tests⁶ with direct heating of the cladding is shown in Fig. 10. W_z is plotted versus burst time. For LOCA test conditions, i.e. short times to burst, in-pile as well as out-of-pile tests result in W_z above 0.5. This means axially localized ballooning.

Microstructural Evaluation of the Cladding Temperature

The Zircaloy-4 microstructure appearance was interpreted in order to estimate the local maximum cladding temperatures reached during the in-pile LOCA transients and to quantify azimuthal temperature differences. For the rods of test series A and B (fresh rods) and the pre-irradiated rods of the test series F evaluated to date, the assessment of the maximum cladding temperature showed good agreement with the TC measurement using type B thermocouples and about 30 to 40 K lower temperatures than type A TCs. Thus the correction value added for the type A TCs seems too high. Azimuthal temperature variations between 0 and 80 K were found.

Cladding Tube Oxidation

The microstructure of the cladding outer surface showed the oxide scale to be dense, adherent, and axially cracked due to clad deformation. Only large deformation led to partial oxide spalling. The continued oxidation after the burst of the cladding formed crack-free, smooth oxide sublayers.

In Fig. 11 the local oxide thickness of the samples from the A, B series and F series (pre-irradiated) is plotted versus the pertinent maximum cladding temperature. The ZrO_2 layer thickness varied between 2 and

8 μm for both, fresh and pre-irradiated rods. This extent of oxidation at the outer cladding surface is comparable to out-of-pile results.^{7, 8}

At the inner surface the oxide layer thickness decreases with increasing distance from the burst opening. The oxidation of the inner tube surface is mainly caused by steam access via the burst opening. No oxide was found more than 100 mm apart from the burst location. The oxide at the inner clad surface appeared smooth and without the strain-induced crack pattern typical for the outer layers. Close to the burst opening the thickness of the inner oxide layer is slightly smaller than the thickness of the outer layer, for fresh rods. However, the pre-irradiated rods of the series F exhibited significantly thicker internal oxide layers compared to the external layer.

Chemical Behavior of the Fuel and the Fission Products

In the in-pile test rods no pronounced chemical interaction between UO_2 fuel and the Zry cladding (internal cladding oxidation by the fuel) occurred during the LOCA transient. Also no influence of fission products, e.g. iodine, on the deformation and rupture behavior has so far been observed. Possibly the iodine was not present in the fuel rod in the proper chemical state since neither preconditioning nor substantial preirradiation of the fuel immediately before the transient were performed. But, the more likely reason could be that in particular iodine is not present at the inner cladding surface at a sufficiently high concentration. The many incipient cracks detected at the inner cladding surface hold for this assumption. A similar crack formation was observed in laboratory tests when the iodine concentration was too low.⁹ The critical iodine concentration depends strongly on temperature. As laboratory tests demonstrated a significant influence of iodine on the burst strain occurs at temperatures below 800 °C only.⁹ But for temperatures above 700 °C the critical iodine concentration required for a low-ductility failure of the Zry tubing due to iodine SCC (stress-corrosion cracking) seems too high to be reached in the in-pile test rods, even under the assumption of a complete iodine release from the high burnup fuel. Since all tested high burnup fuel rods (35,000 MWD/tj) burst at temperatures above 700 °C (730 - 900 °C) the probability for a low-ductility failure of the cladding due to SCC is rather low.¹⁰

Fission Gas Release and Fuel Swelling

The fission gas release from UO_2 and the fuel swelling were determined at the test rods after the pre-irradiation, i.e. without LOCA transient testing, and at the pre-irradiated rods being exposed to the transients. During the steady-state preirradiation of the fuel rods the fission gas release was always below 10 %. During the LOCA transient the additional fission gas release was smaller than 6 %. The release is primarily caused by microcrack formation without the fuel. The various fission gas fractions, i.e. the released gas, the gas in pores, and the gas in the matrix, in fuel samples of the test series F after different treatment are given in Fig. 12. The fuel density increased during irradiation up to about 3 % burnup. This is due to a volume-averaged swelling rate of about 1 % per % burnup and an irradiation-induced densification to about 2 % residual porosity. There was no noticeable swelling during the LOCA-tests.

MAJOR RESULTS AND CONCLUSION

From the test rod data evaluated to date the following results are summarized:

- All pressurized rods ruptured during the heatup phase.
- All ballooned rods exhibit circumferential strains over their entire heated length. The deformation profile was influenced by the axial power profile and locally by the thermocouples.
- All specimens burst at the location of maximum strain and this maximum deformation is located at or near the peak power position.
- The burst data, i.e. burst temperature, burst pressure, and burst strain are similar to results from various out-of-pile tests. No influence of burnup on the burst data was detected.
- The tests with pre-irradiated rods resulted in fragmented fuel pellets in the rod sections with major deformation. The pellet fragments relocated outward and downward filling the space in the fuel rod created by the radial clad deformation.
- Fuel pellet fragmentation does not seem to have affected the cladding deformation process.
- The evaluated data of the radial-strain and axial-strain localization parameter are comparable for fresh and preirradiated fuel rods.
- Microstructural evaluation of the maximum cladding temperature indicated azimuthal temperature differences between 0 and 80 K.
- Steam oxidation of the cladding outer surface is comparable to out-of-pile results. Enhanced local oxidation was observed in some cases with pre-irradiated fuel rods.
- The internal oxide layers observed near the burst position were caused by the steam access via the rupture opening and exhibit a similar thickness compared to the outer surface. Preirradiated tubes show thicker oxide layers on the inside surface compared to unirradiated specimens.
- No influence of fission products on the burst strain of the tubing has so far been detected.
- The fission gas release during the LOCA transient was detected to be smaller than 6 %. It is primarily caused by microcrack formation in the fuel. The swelling of the fuel was negligible.

With respect to the test objectives it may be concluded tentatively that the results available at this time do not indicate a systematic influence of the nuclear environment on fuel behavior under the conditions of these tests.

REFERENCES

1. B.H. CHAPMAN, "Multirod Burst Test Program Progress", Report for January - March 1978, NUREG / CR - 0225, ORNL / NUREG / TM-217, August 1978
2. F. ERBACHER, "Verhalten der Brennelemente beim Kühlmittelverlust-Störfall und Wechselwirkung mit der Kernnotkühlung", KfK 2691, Sept. 1978
3. F. ERBACHER, H.J. NEITZEL, and K. WIEHR, "Deformation Mechanism of Zircaloy Fuel Cladding in a LOCA and Interaction with the Emergency Core Cooling, *Trans. Am. Nucl. Soc.*, 31:336-339 (1979)
4. A.A. BAUER et al., "Evaluating Strength and Ductility of Irradiated Zircaloy", Quarterly Progress Report January - March, 1978, NUREG / CR-0085, BMI-2000, June 1978
5. H.W. CHUNG and T.F. KASSNER, "Deformation Characteristics of Zircaloy Cladding in Vacuum under Steam and Transient Heating Conditions", Summary Report ANL-77-31, July 1978.
6. R.N. ROSE, C.A. MANN, and E.D. HINDLE, "Axial distribution of deformation in the cladding of pressurized water reactor fuel rods in a loss-of-coolant accident", *Nucl. Technol.* 46, 2 (220-227) Dec. 1979
7. S. LEISTIKOW, G. SCHANZ, and H.v. BERG, "Kinetik und Morphologie der isothermen Dampf-Oxidation von Zircaloy-4 bei 700 - 1300 °C", KfK 2587, March 1978
8. S. LEISTIKOW, G. SCHANZ, and H.v. BERG, "Untersuchungen zur temperaturtransienten Dampfoxidation von Zircaloy-4-Hüllmaterial unter hypothetischen DWR-Kühlmittelverlust-Störfallbedingungen", KfK 2810, April 1979
9. P. HOFMANN, J. SPINO, "Influence of Simulated Fission Products on the Ductility and Time-to-Failure of Zircaloy-4 Tubes in LWR Transients", KfK 3054, 1980
10. E.R. KARB et al., "KfK In-pile Tests on LWR Fuel Rod Behavior During the Heatup Phase of a LOCA", KfK 3028, Oct. 1980

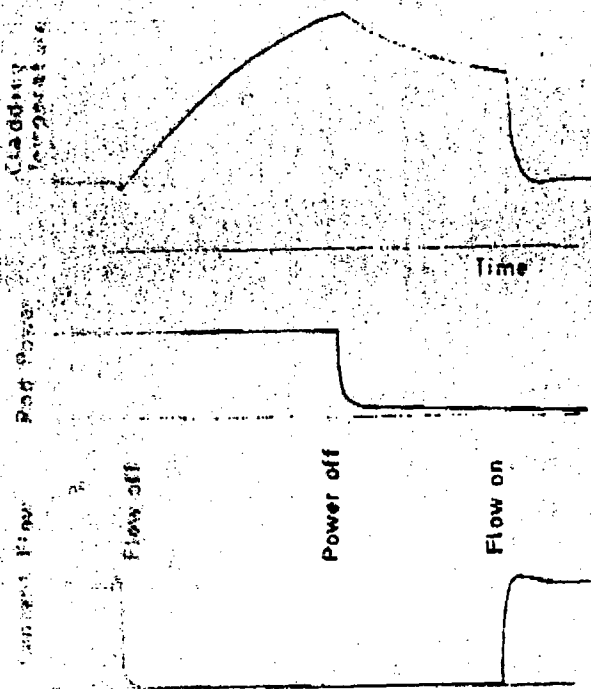


Fig. 1
Test procedure, schematic

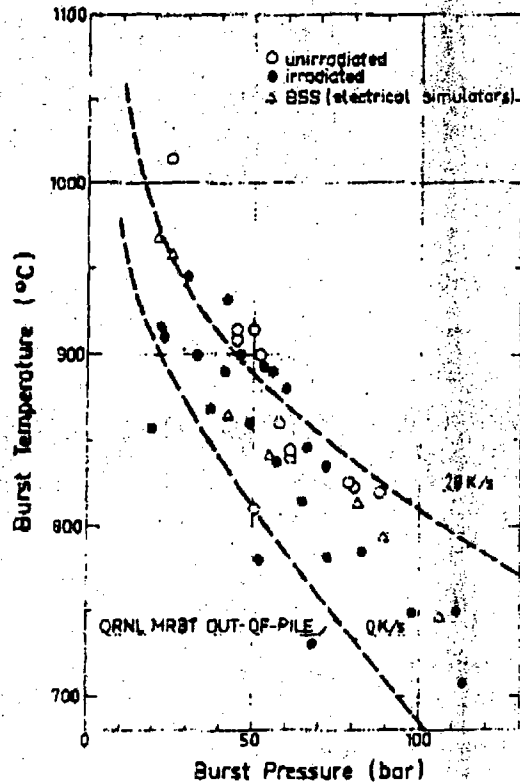


Fig. 2
Burst temperature vs. burst pressure

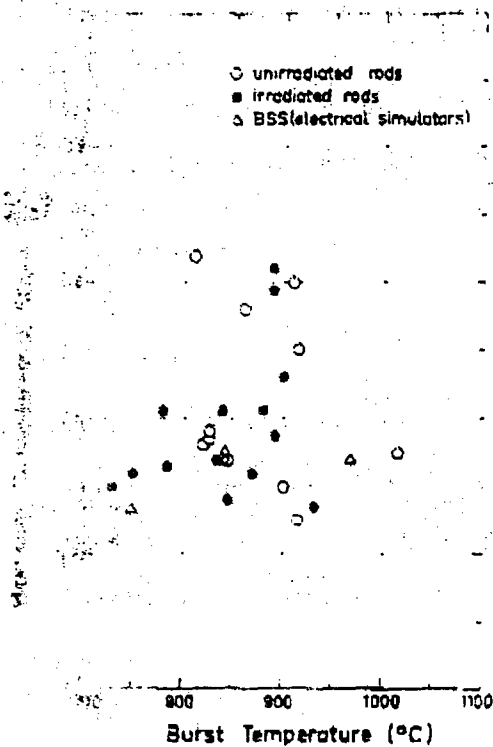


Fig. 3
Max. circumferential strain vs. burst temperature

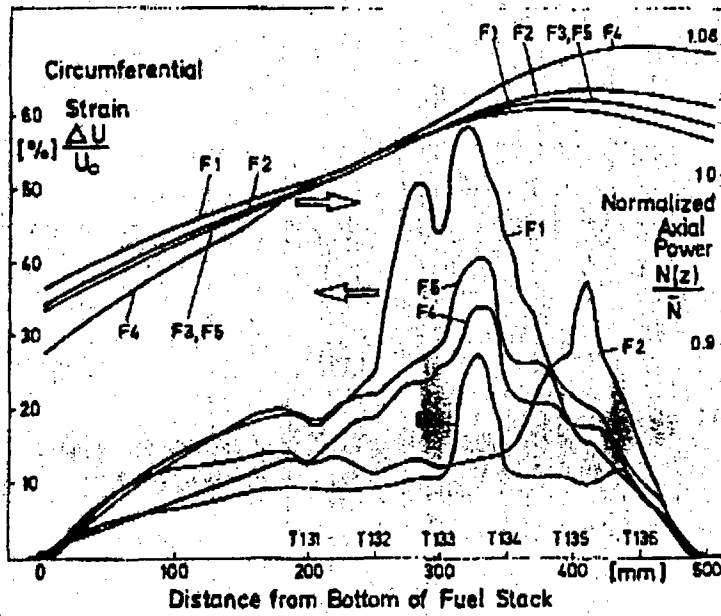


Fig. 4

Circumferential strains and axial power profiles, F1 through F5

Fig. 5

Circumferential strains and axial power profiles A and B tests (unirradiated)

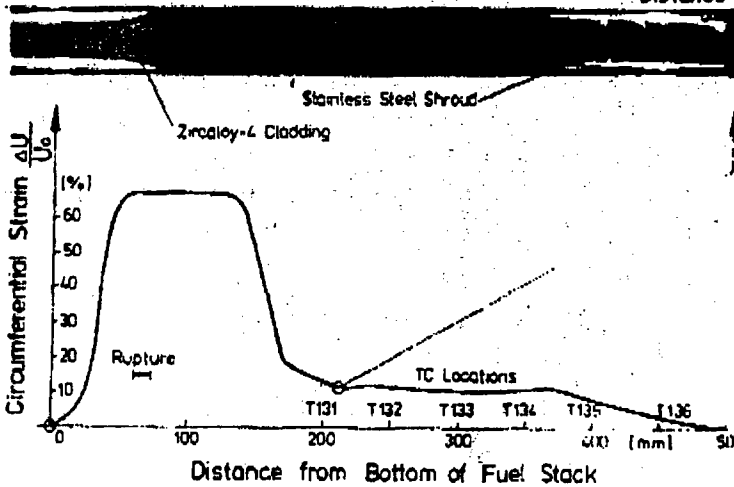
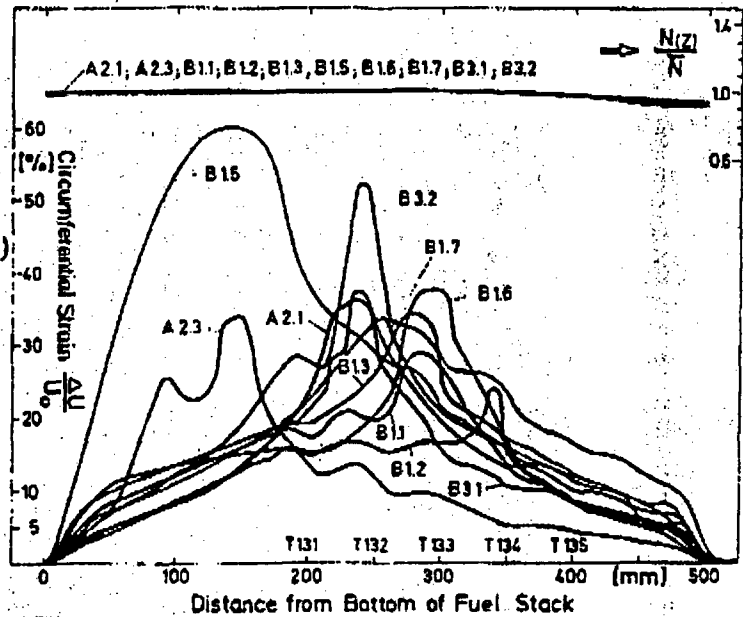


Fig. 6

Posttest neutron radiograph and deformation profile E5

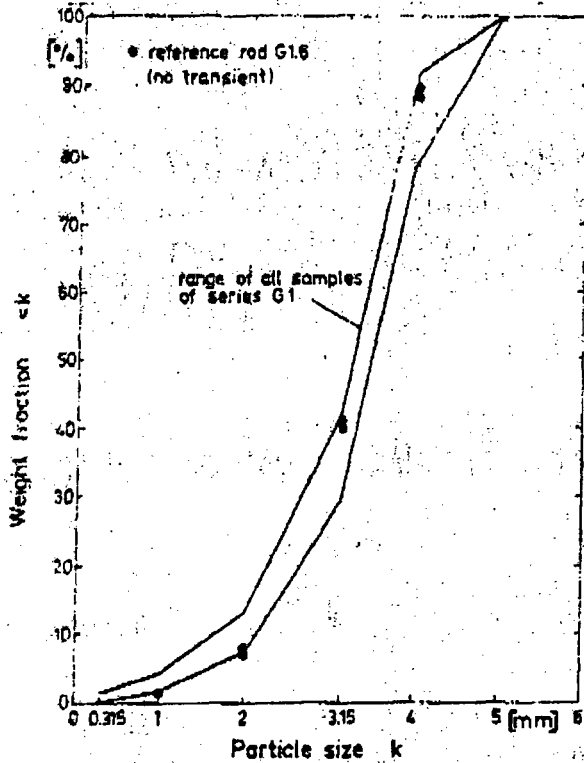


Fig. 7

Fuel particle size distribution, sieve analyses of series G1

Fig. 8

Temperature and internal pressure histories during test E4

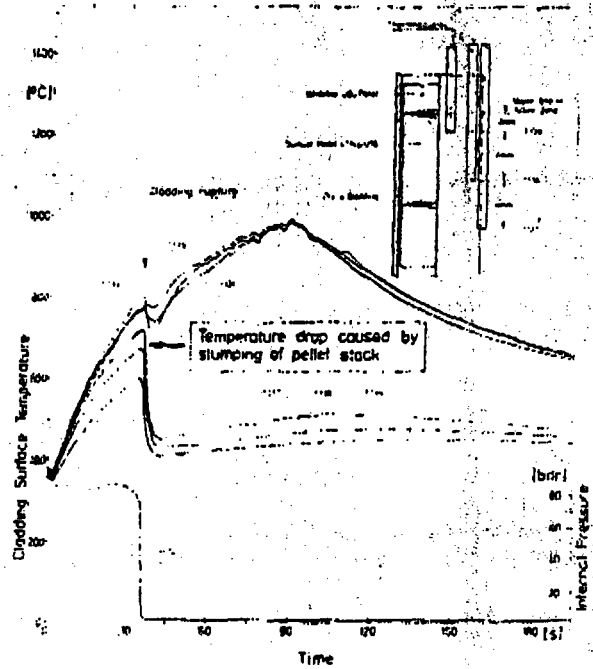
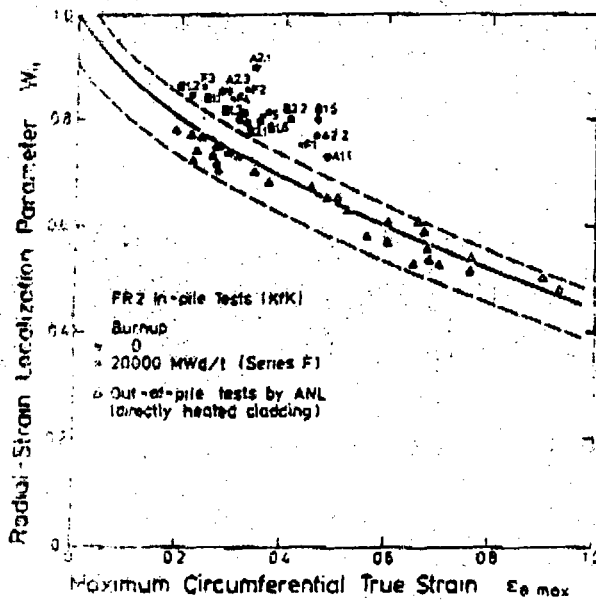


Fig. 9

Comparison of FR2 in-pile tests with ANL out-of-pile data with respect to the radial-strain localization parameter.



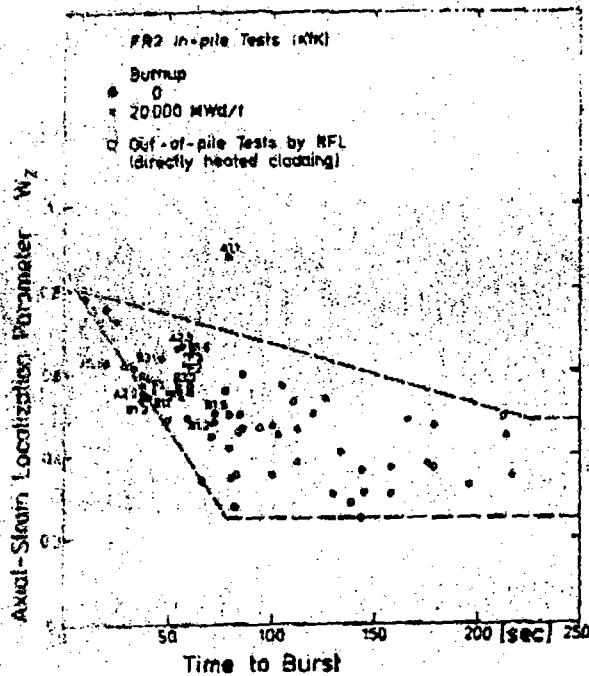


Fig. 10

Comparison of FR2 in-pile tests with out-of-pile data with respect to the axial-strain localization parameter.

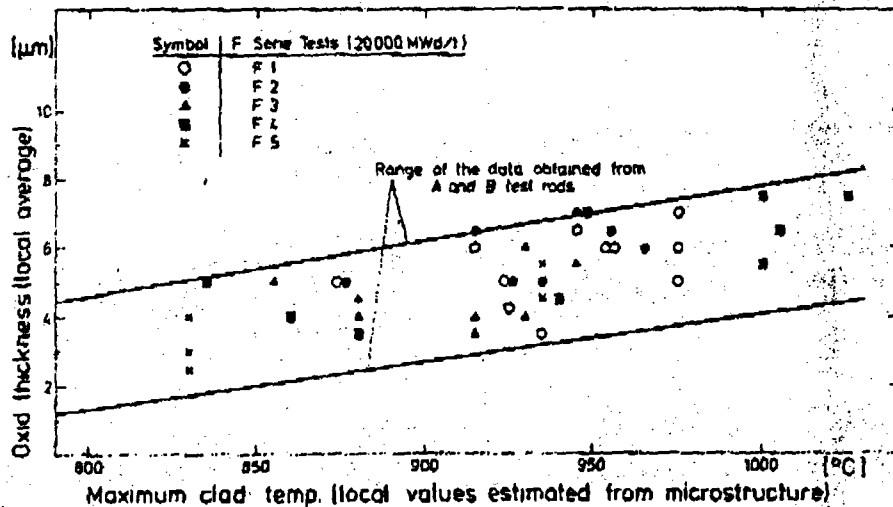


Fig. 11

Stream oxidation of the cladding (outer surface)

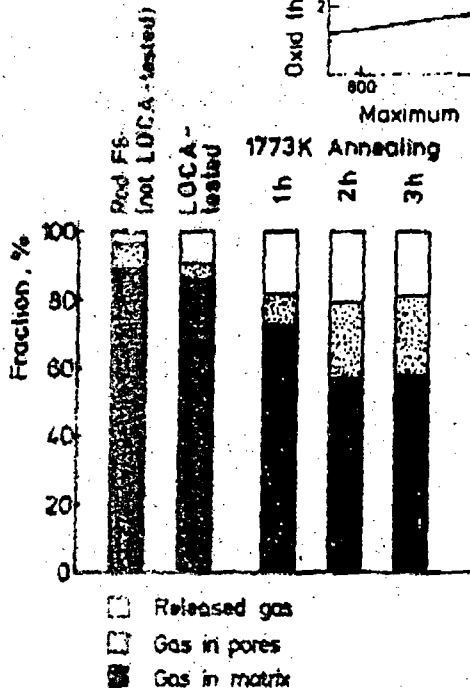


Fig. 12

Fission gas fractions in fuel samples of the test series F (20,000 MWd/t_y)